Golden spiral photonic crystal fiber: polarization and dispersion properties

Arti Agrawal, N. Kejalakshmy, J. Chen, B. M. A. Rahman,* and K. T. V. Grattan

School of Engineering and Mathematical Sciences, City University London, London, EC1V 0HB, United Kingdom

**Corresponding author: b.m.a.rahman@city.ac.uk*

Received September 12, 2008; accepted October 7, 2008; posted October 21, 2008 (Doc. ID 101543); published November 14, 2008

A golden spiral photonic crystal fiber (GS-PCF) design is presented in which air holes are arranged in a spiral pattern governed by the golden ratio, where the design has been inspired by the optimal arrangement of seeds found in nature. The birefringence and polarization properties of this fiber are analyzed using a vectorial finite-element method. The fiber that is investigated shows a large modal birefringence peak value of 0.016 at an operating wavelength of 1.55 μm and exhibits highly tuneable dispersion with multiple zero dispersion wavelengths and also large normal dispersion. The GS-PCF design has identical circular air holes that potentially simplify fabrication. In light of its properties, the GS-PCF could have application as a highly birefringent fiber and in nonlinear optics, and moreover the 2D chiral nature of the pattern could yield exotic properties.

OCIS codes: 060.5295, 060.4370, 060.2400.

The flexibility in the potential for the design of the microstructure of photonic crystal fibers (PCFs) allows for the creation of unique waveguiding properties that are difficult to achieve with conventional single-mode fibers. In the PCF, a high-index silica core is surrounded by a silica cladding that has a lower average index owing to the presence of air holes, and modified total internal reflection guides light in the core. This type of PCF has a large index contrast, and coupled with the freedom to tailor the arrangement and shape of air holes, it is possible to obtain a wide variety of desired polarization and waveguide dispersion behavior.

Highly birefringent fibers have several application areas: high-bit-rate communication systems, gyroscopes, sensing, and in fiber lasers with single-polarization output. PCF designs with large birefringence typically rely on the asymmetry of either the core or of the cladding. In the first approach, double or triple defects may form the core [1,2], two central air holes may be enlarged [3], and a microstructure may be introduced in the core [4]. The second approach introduces asymmetry in the cladding through elliptical air holes [5,6]. A combination of both these approaches may also be used [7]. The birefringence in these structures can reach magnitudes of the order of 10^{-2} [4,6,7]. However, the complicated arrangement of air holes [7] of different sizes and/or shapes [3,4] makes fabrication challenging. In this Letter, a golden spiral photonic crystal fiber (GS-PCF) design is presented in which all the air holes are identical and circular in shape, yet the PCF exhibits a large birefringence of 0.016 at operating wavelength 1.55 μm.

Figure 1 shows the distribution of air holes in the GS-PCF, which has been designed to mimic the arrangement of seeds in a sunflower. The air holes are at a distance of $r_o\sqrt{n}$ from the center, where n is the hole number and r_o is the spiral radius. The defect or missing air hole (numbered as hole 1) is the center of the structure. The distance between consecutively numbered air holes is nearly constant, and each hole is rotated by approximately 1.618 (the golden ratio) revolutions or 61.8% of a complete turn from the previous one. The design lacks rotational symmetry; therefore there is no degeneracy of modes. A golden spiral arrangement has been explored in the context of optical waveguides previously [8], and it was found that the diffraction pattern of such a design consists of circular Bragg rings. Owing to isotropy of the diffraction pattern, coupling into and out of such a fiber would not be affected by mode shape and direction, and this would allow for low-loss coupling of the GS-PCF with other devices. In that work the authors did not consider index guidance, nor did they explore the birefringence and dispersion properties, important issues that are presented here.

In this work, a full-vectorial finite-element method has been used to compute the birefringence, which is defined as the difference in the effective indices of the two orthogonal polarization modes of the GS-PCF. The number of air holes is kept constant at 43 in the numerical experiments reported, unless stated otherwise. The Sellmeier equation has been used to obtain

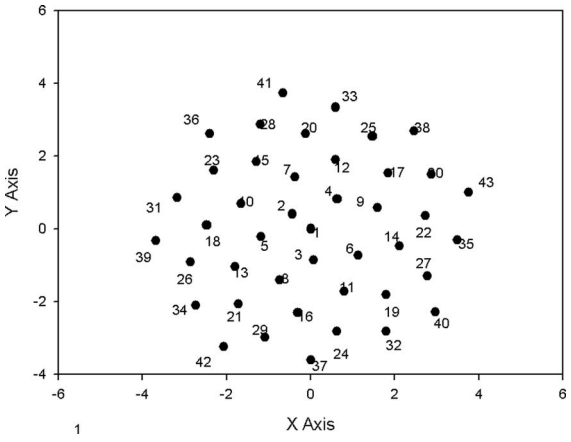

Fig. 1. Distribution of air holes in the GS-PCF.

the refractive index of silica at different wavelengths to account for the material dispersion in computing the total dispersion of the fiber. About 65,000 first order triangular elements arranged in an irregular mesh with 459,617 nodal points have been used to simulate the GS-PCF structure. A single simulation run on a 64-bit quad-core Intel Pentium desktop computer took about 100 s.

First, the effect of the spiral radius on the birefringence is studied as a function of number of air holes in the structure. Figure 2 shows the birefringence variation with number of air holes for a fixed air-filling fraction, $d/r_o=0.8$ at operating wavelength 1.55 μm (where d is the air-hole radius). The birefringence change is almost negligible as the number of air holes in the cladding increases. This shows that asymmetry in the air hole arrangement near the core area causes the large birefringence. The largest birefringence is achieved in the design with the smallest spiral radius because for larger spiral radii the air holes are farther apart, and the field is more confined in a larger core and does not interact strongly with the nearby air holes. As the spiral radius (and hence the distance between air holes) reduces, the field is influenced to a greater degree by the first few air holes that surround the core, and since this air hole arrangement is asymmetric (see Fig. 2 inset) the birefringence increases.

The effect of the air-filling fraction on the birefringence as a function of wavelength has been studied by changing the air-hole radius (d) for a fixed value of spiral radius and is shown in Fig. 3. The birefringence increases with d and also initially with the wavelength. At a fixed wavelength the birefringence is largest for the structure with biggest air holes; the birefringence has a peak value of 0.016 at an operating wavelength of 1.55 μm for parameters $r_o=0.45$ μm, $d=0.36$ μm. Larger air holes lead to a reduced core size and exaggerate the structural asymmetry experienced by the field, resulting in larger birefringence. It can be seen from Fig. 3 that after the birefringence reaches a peak value as the wavelength increases further, the birefringence decreases slightly. At shorter wavelengths the spot size is small (0.901 μm^2 at 0.81 μm), the field is well confined, and when the wavelength increases the expanding field is more affected by the asymmetry of the air holes closest to the core. At larger wavelengths the spot size increases (1.673 μm^2 at 1.55 μm, and 2.889 μm^2 at 1.91 μm) and the field begins to spread farther out, interacting with a larger number of air holes for which the arrangement is more symmetric, and hence the birefringence decreases somewhat.

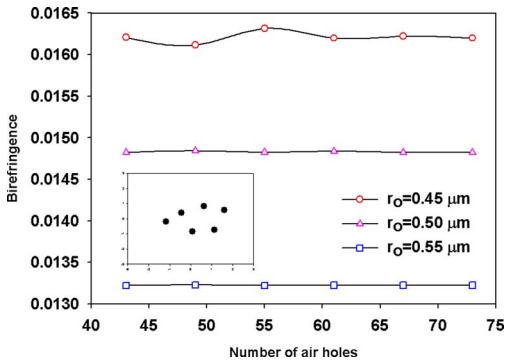

Fig. 2. (Color online) Change in birefringence with the number of the air holes.

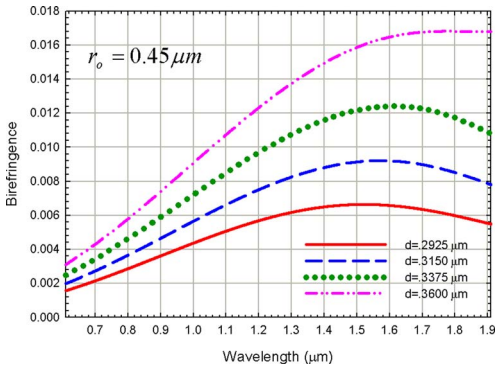

Fig. 3. (Color online) Birefringence as a function of wavelength for fixed spiral radius and changing air-hole radius.

Chromatic dispersion plays an important role in controlling the nonlinear behavior of a fiber. The efficiency of nonlinear effects such as four-wave mixing, the Raman effect, soliton formation/fission, and supercontinuum generation (SCG) can be controlled in a PCF by engineering the fiber design for suitable waveguide dispersion [9] as well as high nonlinearity. The GS-PCF has a very high nonlinear coefficient $\gamma \sim 72.69\ \mathrm{W^{-1}\,K\,m^{-1}}$ for $r_o=0.45$ μm, $d=0.36$ μm owing to a small core area (where $\gamma=2\pi n_2/(\lambda A_{\mathrm{eff}})$, $n_2=3\times10^{-20}\ \mathrm{m^2/W}$) at an operating wavelength of 1.55 μm. The GS-PCF exhibits highly tuneable dispersion that can be altered by changing the spiral and air-hole parameters. Figure 4 shows the total dispersion of the two orthogonal polarizations of the GS-PCF. The dispersion curves have two zero crossings, and the locations of these zero-dispersion wavelengths (ZDWs) are different for the x- and y-polarized modes, allowing for the possibility of single-polarization fiber lasers as well as polarization-controlled SCG. Figure 5 shows the dispersion versus wavelength curves for different values of spiral and air-hole radii such that their ratio is kept fixed at 0.8. It can be seen from Fig. 5 that the GS-PCF can have very large normal dispersion over a broad wavelength range, which would be useful for broadband dispersion compensation [10]. Through an

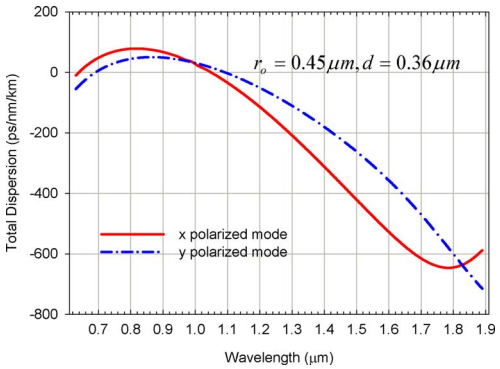

Fig. 4. (Color online) Dispersion variation of the two orthogonal polarizations with wavelength.

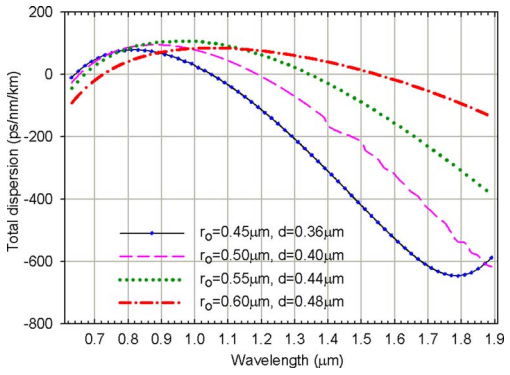

Fig. 5. (Color online) Dispersion as a function of wavelength for an air-filling fraction 0.8.

appropriate choice of air-hole diameter and spiral radius, the dispersion can also be made anomalous with two ZDWs (the second ZDW is ~1.064 μm for r_o=0.45 μm, d=0.36 μm, while the second ZDW is ~ 1.55 μm for r_o=0.6 μm, d=0.48 μm), which can be tuned for nonlinear applications such as SCG [9]. The dispersion variation in this case may be explained thus: for larger r_o, the air holes are farther apart and the core area is larger, leading to a larger effective index that is close to the core index. The field is well spread compared to a smaller value of r_o; therefore the change in the modal effective index with wavelength is smaller, and the dispersion curve has a smaller slope. Also, the long-wavelength behavior (and the second ZDW) is redshifted, because the field interacts with the air holes at comparatively longer wavelengths owing to the larger length scale of the structure. As the air-hole radius and spiral radius decrease, the modal, effective index also decreases and comes closer to the index of the fundamental space filling mode, which is a strong function of wavelength and has large waveguide dispersion variation [11]. Thus, the dispersion can be tuned by changing the wavelength range in which the field interacts strongly with the air holes through changes in the design parameters and changing the rate of decrease of the modal effective index.

The arrangement of air holes in the GS-PCF design does not possess rotational and translational symmetry and is 2D chiral in nature. The sense of rotation of the structure changes when viewed from opposite directions unlike a 3D chiral structure such as a helix. Recently experimental and theoretical studies ([12,13], and references therein) have shown that planar chiral materials can modulate the intensity of light and change the polarization state. The intensity modulation and polarization rotation/elliptization effects change with the direction of the incident light as well as the handedness of the material. This leads to the intriguing possibility of nonreciprocal optical structures and polarization-sensitive devices made of dielectric materials. So far these studies have focused on using planar materials that have been patterned. The GS-PCF offers the possibility of investigating these phenomena in three dimensions in a dielectric medium at telecommunication wavelengths.

In conclusion, the birefringence and dispersion properties of the GS-PCF have been presented. The design is simple and may be easily fabricated by extrusion or drilling technique and can yield very large birefringence with a simple structure comprising only identical circular air holes. The GS-PCF described has tuneable dispersion and can be used to obtain large normal dispersion or anomalous dispersion with multiple adjustable ZDWs. The possibility of exploiting the 2D chiral nature of the GS-PCF for nonreciprocal optical dielectric devices at telecom wavelengths has also been discussed.

References

1. T. P. Hansen, J. Broeng, S. E. B. Libori, E. Knudsen, A. Bjarklev, J. R. Jensen, and H. Simonsen, IEEE Photon. Technol. Lett. **13**, 588 (2001).
2. M. Antkowiak, R. Kotynski, T. Nasilowski, P. Lesiak, J. Wojcik, W. Urbanczyk, F. Berghmans, and H. Thienpont, J. Opt. A **7**, 763 (2005).
3. K. Suzuki, H. Kubota, S. Kawanishi, M. Tanaka, and M. Fujita, Opt. Express **9**, 676 (2001).
4. D. Chen and L. Shen, IEEE Photon. Technol. Lett. **19**, 185 (2007).
5. M. J. Steel and R. M. Osgood, Jr., Opt. Lett. **26**, 229 (2001).
6. Y. Yue, G. Kai, Z. Wang, T. Sun, L. Jim, Y. Lu, C. Zhang, J. Liu, Y. Li, Y. Liu, S. Yuan, and X. Dong, Opt. Lett. **32**, 469 (2007).
7. D. Chen and L. Shen, J. Lightwave Technol. **25**, 2700 (2007).
8. Mesophotonics Limited, "Photonic crystal waveguide," U.S. patent 6,775,448 (August 10, 2004).
9. J. M. Dudley, G. Genty, and S. Coen, Rev. Mod. Phys. **78**, 1135 (2006).
10. L. P. Shen, W.-P. Huang, G. X. Chen, and S. S. Jian, IEEE Photon. Technol. Lett. **15**, 540 (2003).
11. N. Kejalakshmy, B. M. A. Rahman, A. Agrawal, T. Wongcharoen, and K. T. V. Grattan, Appl. Phys. B **93**, 223 (2008).
12. W. Zhang, A. Potts, A. Papakostas, and D. M. Bagnall, Appl. Phys. Lett. **86**, 231905 (2005).
13. V. A. Fedotov, P. L. Mladyonov, S. L. Prosvirnin, A. V. Rogacheva, Y. Chen, and N. I. Zheludev, Phys. Rev. Lett. **97**, 167401 (2006).